Proceedings of IMECE 2006
ASME International Mechanical Engineering Conference and Exhibition
November 5-10, 2006, Chicago, USA

IMECE2006-13590

MOLECULAR DYNAMICS PREDICTION OF THE THERMAL RESISTANCE OF SOLID-SOLID INTERFACES IN SUPERLATTICES

A. J. H. McGaughey*
Department of Mechanical Engineering
Carnegie Mellon University
Pittsburgh, Pennsylvania 15217
Email: mcgaughey@cmu.edu

J. Li
Department of Materials Science and Engineering
The Ohio State University
Columbus, Ohio 43210
Email: li.562@osu.edu

ABSTRACT

Molecular dynamics simulations are used to predict the thermal resistance of solid-solid interfaces in crystalline superlattices using a new Green-Kubo formula. The materials on both sides of the interfaces studied are modeled with the Lennard-Jones potential and are only differentiated by their masses. To obtain the interface thermal resistance, a correlation length in the bulk materials is first obtained, which approaches a system-size independent value for larger systems. The interface thermal resistance is found to initially increase as the layer length is increased, and then to decrease as the phonon transport shifts from a regime dominated by ballistic transport to one dominated by diffusive transport.

NOMENCLATURE

A area
E energy
$\mathbf{F}$ force vector
k thermal conductivity
k_B Boltzmann constant
L length
m mass
$\mathbf{r}$ particle position vector, particle separation vector
q planar energy flux
R thermal resistance
R_m mass ratio
S, $\mathbf{S}$ heat current, heat current vector
t time
T temperature
$\mathbf{v}$ particle velocity vector
V volume
x position

Greek

Δ length
λ correlation length
ϕ potential energy
Φ spatial correlation function

Subscripts

A material on one side of interface
A|B A–B interface
B material on other side of interface
i summation index, particle label
j summation index, particle label
K Kapitza
l direction (x, y, or z)
SL superlattice
x composition fraction

Superscripts

o time average value
∞ large system limit

*Address all correspondence to this author.

INTRODUCTION

A superlattice is a periodic composite material composed of layers of metals, semiconductors, and/or insulators. Superlattices built from group IV semiconductors (e.g., Si/Si$_x$Ge$_{1-x}$) and Group III-V semiconductors (e.g., AlAs/GaAs) have received considerable attention due to their relevance to the electronics industry. By appropriate choice of the layer compositions (including doping) and thicknesses, it is possible to separately control the transport of electrons and phonons in a superlattice [1]. While the electron transport has been considered extensively, attention has only recently turned to the thermal transport characteristics. The potential anisotropy of the superlattice thermal conductivity tensor may be advantageous in systems where the careful control of heat transfer is needed, and superlattices with low thermal conductivity are of interest in thermoelectric energy conversion applications [2].

Thermal transport modeling in superlattices has typically focused on the prediction of the effective thermal conductivity [3–12]. Here, we report on a molecular dynamics (MD) study aimed at predicting the thermal resistance of the interfaces in a model superlattice. The interface resistance plays an important role in the thermal behavior of many of the new nanocomposites being developed. Prediction of its magnitude is challenging, especially when system interfaces are close together, but is crucial for the development of superlattice design techniques.

The nature of phonon transport in a superlattice is first reviewed, followed by a description of modeling methods available. We then propose a method to predict the interface thermal resistance using a Green-Kubo formula, and examine the effects of changing the period length in a superlattice modeled with the Lennard-Jones (LJ) potential.

PHONON TRANSPORT IN SUPERLATTICES

Consider a superlattice composed of layers of equal thickness of materials A and B with a period length L (i.e., $L_{\rm A} = L_{\rm B} = L/2$), as shown in Fig 1. From a continuum standpoint, the thermal resistance normal to the layers of one period of such a structure will be

$$R_{SL} = \frac{L_{\rm A}}{k_{\rm A}} + \frac{L_{\rm B}}{k_{\rm B}} + 2R_{\rm A|B}, \qquad (1)$$

where k_i is the bulk thermal conductivity of material i (i =A,B) and $R_{\rm A|B}$ is the thermal resistance of the A|B interface. Note that $R_{\rm A|B}$ is equal to $R_{\rm B|A}$. As the period length increases, the contribution of $R_{\rm A|B}$ to R_{SL} will decrease, and beyond a certain size, will be negligible. When the interfaces are far enough apart to be considered isolated, the interface thermal resistance can also be called the Kapitza resistance, $R_{\rm K,A|B}$.

To move from the continuum description of Eq. (1) to the nanoscale superlattices currently being fabricated, we must consider the nature of the phonon transport as L decreases. When the superlattice period is large (i.e., greater than the bulk phonon mean free path of the constituent species), phonons that leave one interface will scatter with other phonons before reaching the next interface. This is diffusive transport, and one can consider the interfaces as being isolated, with most of the phonon transport occurring in a bulk-like manner. Additionally, all phonons incident on the interface are scattered. This behavior is known as incoherent phonon transport, in that the vibrational modes in the different layers are distinct. Isolated interfaces are the type most generally modeled [13–19].

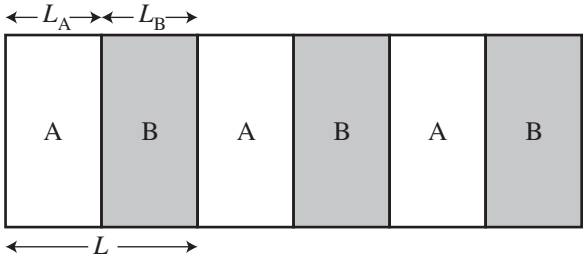

Figure 1. MODEL SUPERLATTICE WITH PERIOD L.

As the period length decreases below the bulk phonon mean free path, some phonons leaving an interface may travel through the entire layer without scattering with other phonons, and be scattered at the next interface. This is ballistic phonon transport, and while the phonons are still incoherent across the interface, the assumption of bulk-like behavior in the layers becomes less valid [i.e., the use of $k_{\rm A}$ and $k_{\rm B}$ in Eq. (1) becomes questionable]. The interfaces are no longer isolated. As the layer thickness gets smaller, the phonon transport will become more ballistic.

When the layer thickness gets smaller still, another transition takes place. At some point, the layers no longer exhibit any behavior typical of their bulk equivalents. The phonon dispersion is now better represented by the superlattice unit cell than by distinct relations in each layer. The phonons are now coherent, in that they do not see the interface as a scattering location, but as part of a new "bulk" material. The phonon transport in this regime is diffusive, and the concept of the interface resistance is no longer applicable. The majority of lattice-dynamics based superlattice thermal conductivity prediction studies have considered such systems [4, 5, 9].

In this investigation, we are concerned with the second of these three regimes, where the phonons are incoherent across the interfaces and the transport in the layers has both diffusive and ballistic components.

INTERFACE THERMAL RESISTANCE PREDICTION

When an energy flux q passes through an interface with area A between materials A and B, a temperature drop ΔT results. The

interface thermal resistance is defined from

$$\frac{q}{A} = -\frac{\Delta T}{R_{\mathrm{A|B}}}, \tag{2}$$

which is similar in form to the Fourier law of conduction.

The simplest models of incoherent interfacial phonon transport are the acoustic mismatch model (AMM) and the diffusive mismatch model (DMM) [20]. In the AMM, the transmission of energy across the interface (which is assumed to be perfect) is dependent on the bulk properties of the two materials. There is no scattering at the interface, just transmission and reflection of energy. The AMM has been found to give good predictions at low temperatures (< 30 K) [21], where the phonon transport is dominated by long-wavelength modes. In the DMM, all phonons are assumed to scatter diffusely at the interface. At a solid-solid interface, diffuse scattering may account for up to 10% of the total scattering [20]. The distribution of energy between the two sides of the interface after a scattering event is based on the phonon density of states and phonon group velocities of the bulk materials. As both the AMM and DMM rely on bulk material properties, they are only strictly valid for isolated interfaces.

Young and Maris [13] developed a more refined approach to model the phonon transport at the interface between two semi-infinite harmonic face-centered cubic (fcc) lattices. Using detailed information about the phonon dispersion obtained from lattice dynamics calculations, specifics about the reflected and transmitted phonon modes can be found and used to predict the interface thermal resistance. For interfaces of materials whose Debye temperatures are within a factor of five, the predictions are in reasonable agreement with experiments [14]. Zhao and Freund [19] extended this method to model phonon transport at the interface between materials with a diamond structure, allowing for examination of acoustic and optional phonons. While this method can provide very detailed information, it is limited by the harmonic nature of the lattice dynamics approach (which may lead to errors as the temperature of the system is increased) and the need to model isolated interfaces.

Molecular dynamics simulations can also be used to investigate interfacial thermal transport. In a MD simulation, the positions and momenta of a system of classical particles are predicted using Newton's second law and an appropriate interatomic potential. One of the advantages of MD simulations is that no *a priori* assumptions about the nature of the thermal transport need to be made. The most commonly used method to predict the interface thermal resistance using MD simulations is called the direct method [6, 10, 15, 17, 18, 22, 23]. A simulation cell long in one dimension is used, and a known heat flux is established between hot and cold reservoirs with controlled temperatures. The interface is placed between the hot and cold reservoirs, and the resulting temperature drop across it and the known heat flux are used to find the interface thermal resistance using Eq. (2). This approach has been used to study grain boundaries in silicon [15, 18] and diamond [23], and for interfaces in LJ systems [6, 10, 22]. Long simulation cells are typically needed to get system-size independent results.

An alternative method to finding the interface thermal resistance in an MD simulation is to use a Green-Kubo approach, where information regarding transport in a system is obtained from equilibrium simulations [24]. In the next section, we modify a GK approach for interfacial transport proposed by Puech *et al*. [25], and apply it to a simple mass-mismatch LJ interface. With the GK method we are able to investigate layer-thickness effects, and gain further insight into the nature of the interfacial transport.

PLANAR FLUX GREEN-KUBO FORMULA FOR THE INTERFACE THERMAL RESISTANCE

Puech *et al.* [25] suggest that the thermal resistance of the interface between materials A and B can be predicted using the Green-Kubo formula

$$\frac{1}{R_{\mathrm{A|B}}} = \frac{1}{A k_{\mathrm{B}} T^2} \int_0^\infty dt \langle q(t) q(0) \rangle, \tag{3}$$

where k_{B} is the Boltzmann constant and $q(t)$ is the flux of energy (the planar flux) though the surface at time t (i.e., the power). The integrand, $\langle q(t)q(0)\rangle$, is the planar flux autocorrelation function (PFACF).

Barrat and Chiaruttini [26] applied this formulation to predict the thermal resistance of a LJ solid-liquid interface using MD simulations. They define the planar flux between two phases A and B as

$$q(t) = \sum_{i \in \mathrm{A}} \sum_{j \in \mathrm{B}} \mathbf{F}_{ij} \cdot \mathbf{v}_i, \tag{4}$$

where the first summation is over all atoms in phase A, the second summation is over all atoms in phase B, $\mathbf{F}_{ij}$ is the force exerted by atom j on atom i, and $\mathbf{v}_i$ is the velocity of atom i. In practice, only atoms within the cutoff radius of the interface need to be considered in the summations. Good agreement is found between the prediction of Eq. (3) and that from a direct method calculation. Shenogin *et al.* [27] used this formulation to investigate the thermal relaxation of fullerenes in liquid octane.

We applied Eq. (3) to a LJ system with an interface where the two materials only differ by their masses (the details are discussed in the next section). An interface thermal resistance one order of magnitude larger than that predicted by Stevens *et al.* [22] (who used the direct method for a similar system) was

found. We reproduced the Stevens *et al* result with our own direct method code (not reported here).

Based on these findings, we propose that a modification to the Puech Green-Kubo formula, Eq. (3), is required. We believe that the error in the original derivation comes when it is assumed that the temperature of material B is spatially uniform, giving it an infinite thermal conductivity (see page 1608 of Ref. [26]). In reality, there will be fluctuations in the B phase temperature due to its finite thermal conductivity and fluctuations in the planar energy flux. The same is true for the A phase. This fact suggests that the regions near the interface play a critical role in the interfacial resistance and may be contributing to the predicted resistance from Eq. (3).

To that end, we propose the following new GK formula for the interface thermal resistance:

$$\frac{1}{R_{\mathrm{A|B}}+(k_{\mathrm{A}}^{-1}\lambda_{\mathrm{A}}+k_{\mathrm{B}}^{-1}\lambda_{\mathrm{B}})/2}=\frac{1}{Ak_BT^2}\int_0^\infty dt\langle q(t)q(0)\rangle, \quad (5)$$

where λ_{A} is a correlation length in perfect bulk A, and similar for λ_{B}. The right hand side of (5) is the same as in Eq. (3). The denominator of the left hand side of Eq. (5) is the series summation of the thermal resistances near and across the A|B interface. Note that Eq. (5) will give a smaller $R_{\mathrm{A|B}}$ than Eq. (3), as we require based on our preliminary findings.

The thermal conductivity of perfect A in the lth direction ($l=x,y,z$) in Eq. (5) can be predicted from the Green-Kubo formula [24]

$$k_{l,\mathrm{A}}=\frac{1}{Vk_{\mathrm{B}}T^2}\int_0^\infty \langle S_l(t)S_l(0)\rangle_{\mathrm{A}}dt, \quad (6)$$

where V is the system volume, $S_l(t)$ is the heat current in direction l, and $\langle\rangle_{\mathrm{A}}$ indicates ensemble averaging in perfect A. The heat current vector can be given by [28]

$$\mathbf{S}=\frac{d}{dt}\sum_i E_i\mathbf{r}_i^o=\frac{1}{2}\sum_{i<j}\mathbf{F}_{ij}\cdot(\mathbf{v}_i+\mathbf{v}_j)\mathbf{r}_{ij}^o, \quad (7)$$

where E_i and $\mathbf{r}_i$ are the total energy and position vector of particle i, $\mathbf{r}_{ij}$ is $\mathbf{r}_i-\mathbf{r}_j$, and the superscript o indicates a time averaged value. The last equality only applies for a pair potential. For the remainder of this paper, we will identify the heat current normal to the interface by $S(t)$.

We propose to evaluate the correlation length for material A as

$$\lambda_{\mathrm{A}}=\frac{\int_0^\infty\langle S(t)S(0)\rangle_{\mathrm{A}}dt}{L\int_0^\infty\langle q(t)q(0)\rangle_{\mathrm{A}}dt}, \quad (8)$$

where $L=V/A$, the length of the simulation cell of perfect A studied. To justify Eq. (8), first define a localized planar energy flux $q(x,t)$ such that

$$S(t)=\int_0^L q(x,t)dx. \quad (9)$$

The planar flux given by Eq. (4) does not satisfy this relation [i.e., it cannot predict Eq. (7)], in that it does not take into account the distance separating the pairs of atoms. Instead, we propose a localized planar flux

$$q(x,t)=\sum_{i<j}\frac{\mathbf{F}_{ij}\cdot(\mathbf{v}_i+\mathbf{v}_j)}{2}(x_i^o-x_j^o)\times \frac{H\left(\frac{x_i^o+x_j^o}{2}-x+\frac{\Delta}{2}\right)H\left(x+\frac{\Delta}{2}-\frac{x_i^o+x_j^o}{2}\right)}{\Delta}, \quad (10)$$

where H is the Heaviside step function, and Δ is a distance chosen so that the center of all bonds considered in the sum falls in the range $(x-\Delta/2,x+\Delta/2)$. This planar flux produces the correct system heat current $S(t)$. We compared the predictions of Eqs. (4) and (10) in a monatomic system and found very good agreement when $\Delta=1$. This result makes sense, as using $\Delta=1$ will give the interactions between the layers of atoms on either side of the interface (which will dominate the flow of energy) the same weight they have in Eq. (4). With $\Delta=1$, the integral of the autocorrelation of the two expressions for the planar flux gives the same converged value [as required in Eq. (3)]. The integral of the autocorrelation of Eq. (10) has an oscillatory component, making its specification more difficult. For this reason, in subsequent analysis we use Eq. (4) for the planar flux, knowing that it will give the same result as Eq. (10).

Substituting Eq. (9) for the heat current into the integral in the GK thermal conductivity formula, Eq. (6), leads to

$$\begin{aligned}&\int_0^\infty\langle S(t)S(0)\rangle_{\mathrm{A}}dt \quad (11)\\ &=\int_0^\infty\langle\int_0^L q(x,t)dx\times\int_0^L q(x',0)dx'\rangle_{\mathrm{A}}dt\\ &=\int_0^L dx\int_0^L dx'\int_0^\infty\langle q(x,t)q(x',0)\rangle_{\mathrm{A}}dt\\ &=L\int_{-L/2}^{L/2}dx\int_0^\infty\langle q(0,t)q(x,0)\rangle_{\mathrm{A}}dt.\end{aligned}$$

The integrand in the last line implies a possible spatial correlation between the planar flux at positions separated by a distance x. To

take such spatial correlations into account, we define

$$\Phi(x) \equiv \frac{\int_0^\infty \langle q(0,t)q(x,0)\rangle_{\mathrm{A}} dt}{\int_0^\infty \langle q(0,t)q(0,0)\rangle_{\mathrm{A}} dt}, \tag{12}$$

where $\Phi(x)$ is even, periodic in x with period L (to account for the periodic boundary conditions in the MD system), and $\Phi(0) = 1$ (i.e., the planar flux at one location is perfectly correlated with itself). Then,

$$\begin{aligned} &\int_0^\infty \langle S(t)S(0)\rangle_{\mathrm{A}} dt \\ &= L \int_0^\infty \langle q(0,t)q(0,0)\rangle_{\mathrm{A}} dt \int_{-L/2}^{L/2} \Phi(x) dx, \end{aligned} \tag{13}$$

and we interpret $\int_{-L/2}^{L/2} \Phi(x)dx$ as the correlation length, λ_{A}, indicating how far spatial correlations in $q(x,t)$ persist. In a bulk system, the quantity $\langle q(x,t)q(x,0)\rangle_{\mathrm{A}}$ will be independent of x.

MOLECULAR DYNAMICS SIMULATIONS

In the following, all reported quantities are dimensionless. We consider systems described by the LJ potential, where the atomic interactions are modeled using the interatomic potential

$$\phi_{ij}(r_{ij}) = 4\left(\frac{1}{r_{ij}^{12}} - \frac{1}{r_{ij}^{6}}\right), \tag{14}$$

where ϕ_{ij} is the potential energy between atoms i and j. The LJ potential has been extensively used to model thermal transport in model systems as a means to developing techniques that can later be applied to more realistic systems [6, 10, 12, 26, 29–32].

All simulations are run at a temperature of 0.3307 and at zero pressure. The equilibrium positions of the atoms correspond to a fcc crystal with lattice constant of 1.5793 [31]. As shown in Fig. 2, the simulation is a rectangular solid. There are four unit cells in each of the y- and z-directions (parallel to the interface), and the number of unit cells in the x-direction is varied. The system contains two layers of equal length in the x-direction, one of material A and the other of material B. All data collected are from simulations run in the NVE ensemble (constant mass, volume, and energy). The time step is 0.002, a potential cutoff of 2.5 is applied, and periodic boundary conditions are imposed in all directions. Further details on the MD methods can be found in Refs. [30] and [31].

Two types of simulation were performed. First, we considered monatomic (A=B) systems with $m_{\mathrm{A}} = m_{\mathrm{B}} = 1$ to find the correlation length needed in Eq. (5). The PFACF was calculated at two imaginary interfaces that divided the simulation cell into two equal parts. Total system lengths between 15.79 and 110.55 were considered (corresponding to simulation cells containing 640 to 4480 atoms).

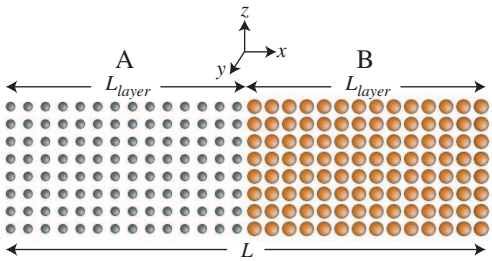

Figure 2. MOLECULAR DYNAMICS SIMULATION CELL. FOR THE CORRELATION LENGTH SIMULATIONS $m_{\mathrm{A}} = m_{\mathrm{B}} = 1$. FOR THE INTERFACE THERMAL RESISTANCE SIMULATIONS, $m_{\mathrm{A}} = 1$ AND $m_{\mathrm{B}} = 2$.

Second, MD simulations of interfacial systems were performed to predict the interface thermal resistance. The materials A and B only differ by their masses. As a result of the periodic boundary conditions, the system contains two identical interfaces. The two materials have the same LJ length and energy scales so that the zero-pressure cell size for the monatomic system can be used. We consider the effects of changing the layer thickness between 6.32 and 55.28 for a mass ratio, R_m, of $m_{\mathrm{B}}/m_{\mathrm{A}} = 2$.

For each system studied, twenty independent simulations were run from random initial conditions to ensure a proper sampling of the system's phase space. In each independent simulation, data were collected over one million time steps. Autocorrelations [as required in Eqs. (3) and (6)] are calculated over 50,000 time steps with a new time origin every five time steps.

CORRELATION LENGTH PREDICTION

To find the correlation length both the numerator and denominator of Eq. (8) must be specified. The numerator is related to the thermal conductivity of the system, and the denominator to the total thermal resistance associated with the interface region. We determine the correlation length for systems with 10, 20, 30, 40, 50, 60, and 70 unit cells in the x-direction. As species A and B are only differentiated by their mass, λ_{A} and λ_{B} are equal.

Thermal Conductivity

The numerator of Eq. (8), $\int_0^\infty \langle S(t)S(0)\rangle_{\mathrm{A}} dt$ is related to the thermal conductivity of material A through Eq. (6). The thermal conductivity for simulation cells long in x-direction and with four unit cells in the y- and z directions is shown in Fig. 3. To specify the thermal conductivity, the integral of the heat current autocorrelation function is fit with the sum of two decaying ex-

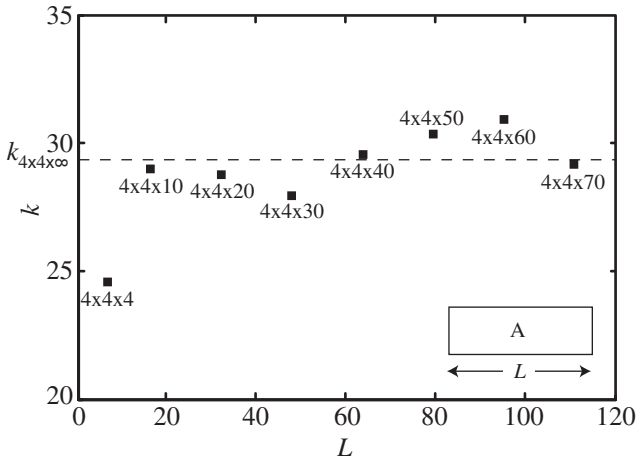

Figure 3. PERFECT A THERMAL CONDUCTIVITY PLOTTED AS FUNCTION OF SYSTEM LENGTH. THE SYSTEM SIZE, IN UNIT CELLS, IS INDICATED FOR EACH POINT.

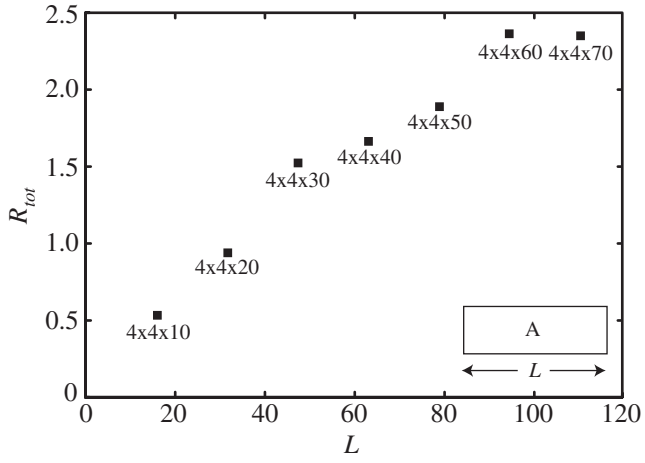

Figure 4. TOTAL THERMAL RESISTANCE NEAR AND ACROSS AN INTERFACE IN THE MONATOMIC SYSTEM PREDICTED BY Eq. (15). THE SYSTEM SIZE, IN UNIT CELLS, IS INDICATED FOR EACH POINT.

ponentials [30]. While the $4 \times 4 \times 4$ value has previously been shown to correspond to the bulk value for cubic systems [31], the non-cubic simulation cell leads to a higher thermal conductivity, saturating by the $4 \times 4 \times 10$ simulation cell. The higher thermal conductivity results from long wavelength phonon modes in the x-direction that have fewer scattering options that they would have in a cubic system. Averaging the thermal conductivity for the seven largest systems shown in Fig. 3, we get $k_{4\times4\times\infty} = 29.4$, the value we will use for systems ten unit cells and longer. In previous investigations, we have assigned an uncertainty of 5% to GK thermal conductivity predictions. The thermal conductivities of the seven long systems are all within 5% of $k_{4\times4\times\infty}$.

Total Thermal Resistance

Define the total resistance, R_{tot}, as that predicted by the Puech GK formula:

$$\frac{1}{R_{tot}} = \frac{1}{Sk_B T^2} \int_0^\infty \langle q(t)q(0)\rangle dt. \tag{15}$$

This quantity is shown in Fig. 4 for an interface in the monatomic system. The integral of the PFACF is obtained directly by averaging the last 10,000 time steps of the autocorrelation data. The total resistance increases with the system size, as correlations between the interface and itself (through periodic boundary conditions) diminish. In theory, the resistance should saturate for large systems. This point is discussed in the next section.

Correlation Length

The correlation length is plotted in Fig. 5. For small systems, the correlation length closely follows the system size, an indication of ballistic phonon transport. As the system size gets bigger,

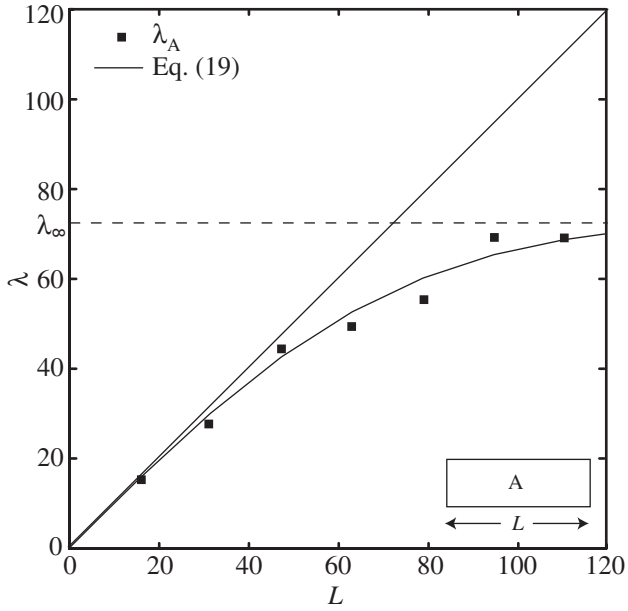

Figure 5. CORRELATION LENGTH PREDICTED FROM Eq. (8) PLOTTED VS. SYSTEM LENGTH.

the correlation length deviates from the system size. Comparing Eqs. (8) and (13), we have

$$\lambda_A^{\text{computed}} = \int_{-L/2}^{L/2} \Phi(x)dx, \tag{16}$$

and, in the large system limit,

$$\lambda_A^\infty = \int_{-\infty}^{\infty} \Phi(x)dx. \tag{17}$$

The correlation lengths predicted from the MD simulations suggest taking $\Phi(x)$ to have a Gaussian shape:

$$\Phi(x) = \exp\left(-\frac{\pi x^2}{\lambda_A^{\infty 2}}\right), \tag{18}$$

where λ_A^∞ is the large system (i.e., isolated interface) correlation length. Then, using Eq. (16), we can predict the correlation length from

$$\lambda_A = \lambda_A^\infty \mathrm{erf}\left(\frac{\pi^{1/2} L}{2\lambda_A^\infty}\right). \tag{19}$$

We obtain λ_A^∞ by fitting Eq. (19) to the MD data, and obtain a value of 72.76. The resulting curve is shown in Fig. 5.

INTERFACE THERMAL RESISTANCE

In this section, we predict the thermal resistance of interfaces in the $R_m = 2$ systems, shown in Fig. 2. To find the interface thermal resistance, the perfect A (or B) quantity needed is λ_A/k_A, which, from Eqs. (6) and (8) reduces to

$$\frac{\lambda_A}{k_A} = \frac{S k_B T^2}{\int_0^\infty \langle q(t)q(0)\rangle_A dt}. \tag{20}$$

The layered systems studied have a maximum thickness of 55.28. In Fig. 6, the R_{tot} values for these systems, and the $R_{A|B}$ values calculated from the new GK formula are plotted as a function of the layer thickness. Also shown in the plot is the value of the interface thermal resistance predicted by Stevens *et al*. [22] using the direct method. The interface resistance ($R_{A|B}$) initially increases, then starts to decrease, and is still decreasing for the largest system size considered. With the value of λ_A^∞ from the previous section, and taking a saturated R_{tot} value of 3.2, an interface resistance of 0.221 is predicted for an infinite system, within 10% of the Stevens *et al*. value of 0.248, found using the direct method for a system with 20 unit cells in each layer (a layer thickness of about 32). In thermal conductivity predictions, size effects in GK and direct method predictions are known to manifest in different ways [33], which seems to be the case here

DISCUSSION AND SUMMARY

We have proposed a new GK formula to predict the thermal resistance of an interface, and applied it to a model LJ solid-solid interface where the two species differ only by their masses.

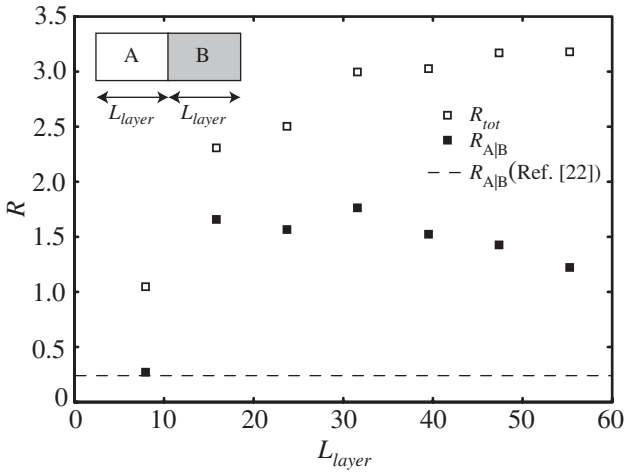

Figure 6. THERMAL RESISTANCES IN THE LAYERED STRUCTURE.

By varying the length of the layers, signs of both ballistic and diffusive phonon transport are evident. In further studies, we will consider systems with more than one layer of materials A and B, to truly simulate a superlattice.

In considering Eq. (5), we can see why Barrat and Chiaruttini [26] found good agreement between the Puech GK formula, Eq. (3), and a direct method prediction. First, the correlation length in a liquid will be small, reducing the resistance associated with the liquid side. Second, the thermal resistance of a liquid-solid interface will be greater than that of a solid-solid interface, so that this term may dominate the denominator of the left side of Eq. (5), and give a similar prediction as Eq. (3). We note that Barrat and Chiaruttini indicate that the integral of the PFACF should show a plateau, then decay monotonically to zero. We do not see such behavior in any of the simulations we performed.

Considerable work is still required in the assessment of the new GK formula for the interface thermal resistance and it's application to superlattices. The size dependence of the correlation length warrants further study, as does the apparent saturation of different quantities (thermal conductivity, total resistance, and interface resistance) at different system sizes. The use of the bulk thermal conductivity for smaller layers in Eq. (5) must also be examined.

REFERENCES

[1] Chen, G., Dresselhaus, M. S., Dresselhaus, G., Fleurial, J.-P., and Caillat, T., 2003. "Recent developments in thermoelectric materials". *International Materials Reviews,* **48**, pp. 45–66.

[2] Kim, W., Zide, J., Gossard, A., Klenov, D., Stemmer, S., Shakouri, A., and Majumdar, A., 2006. "Thermal conductivity reduction and thermoelectric figure of merit in-

crease by embedding nanoparticles in crystalline semiconductors". *Physical Review Letters,* **96**, p. 045901.

[3] Simkin, M. V., and Mahan, G. D., 2000. "Minimum thermal conductivity of superlattices". *Physical Review Letters,* **84**, pp. 927–930.

[4] Bies, W. E., Radtke, R. J., and Ehrenreich, H., 2000. "Phonon dispersion effects and the thermal conductivity reduction in GaAs/AlAs superlattices". *Journal of Applied Physics,* **88**, pp. 1498–1503.

[5] Yang, B., and Chen, G., 2001. "Lattice dynamics study of anisotropic heat conduction in superlattices". *Microscale Thermophysical Engineering,* **5**, p. 107.

[6] Abramson, A. R., Tien, C.-L., and Majumdar, A., 2002. "Interface and strain effects on the thermal conductivity of heterostructures: A molecular dynamics study". *Journal of Heat Transfer,* **124**, p. 963.

[7] Daly, B. C., Maris, H. J., Imamura, K., and Tamura, S., 2002. "Molecular dynamics calculation of the thermal conductivity of superlattices". *Physical Review B,* **66**, p. 024301.

[8] Daly, B. C., Maris, H. J., Tanaka, Y., and Tamura, S., 2003. "Molecular dynamics calculation of the in-plane thermal conductivity of GaAs/AlAs superlattices". *Physical Review B,* **67**, p. 033308.

[9] Broido, D. A., and Reinecke, T. L., 2004. "Lattice thermal conductivity of superlattice structures". *Physical Review B,* **70**, p. 081310(R).

[10] Chen, Y., Li, D., Yang, J., Wu, Y., Lukes, J. R., and Majumdar, A., 2004. "Molecular dynamics study of the lattice thermal conductivity of Kr/Ar superlattice nanowires". *Physica B,* **349**, pp. 270–280.

[11] Dames, C., and Chen, G., 2004. "Theoretical phonon thermal conductivity of Si/Ge superlattice nanowires". *Journal of Applied Physics,* **95**, pp. 682–693.

[12] Chen, Y., Li, D., Lukes, J. R., Ni, Z., and Chen, M., 2005. "Minimum superlattice thermal conductivity from molecular dynamics". *Physical Review B,* **72**, p. 174302.

[13] Young, D. A., and Maris, H. J., 1989. "Lattice-dynamical calculation of the Kapitza resistance between fcc lattices". *Physical Review B,* **40**, pp. 3685–3693.

[14] Stoner, R. J., and Maris, H. J., 1993. "Kapitza conductance and heat flow between solids at temperatures from 50 to 300 k". *Physical Review B,* **48**, pp. 16373–16387.

[15] Maiti, A., Mahan, G. D., and Pantelides, S. T., 1997. "Dynamical simulation of nonequilibrium processes - heat flow and the Kapitza resistance across grain boundaries". *Solid State Comminications,* **102**, pp. 517–521.

[16] Schelling, P. K., and Phillpot, S. R., 2003. "Multiscale simulation of phonon transport in superlattices". *Journal of Applied Physics,* **93**, pp. 5377–5387.

[17] Twu, C.-J., and Ho, J.-R., 2003. "Molecular-dynamics study of energy flow and the Kapitza conductance across an interface with imperfection formed by two dielectric thin films". *Physical Review B,* **67**, p. 205422.

[18] Schelling, P. K., Phillpot, S. R., and Keblinski, P., 2004. "Kapitza conductance and phonon scattering at grain boundaries by simulation". *Journal of Applied Physics,* **95**, pp. 6082–6091.

[19] Zhao, H., and Freund, J. B., 2005. "Lattice-dynamical calculation of phonon scattering at ideal Si-Ge interfaces". *Journal of Applied Physics,* **97**, p. 024903.

[20] Swartz, E. T., and Pohl, R. O., 1989. "Thermal boundary resistance". *Review of Modern Physics,* **61**, pp. 605–668.

[21] Swartz, E. T., and Pohl, R. O., 1987. "Thermal resistance of interfaces". *Applied Physics Letters,* **51**, pp. 2200–2202.

[22] Stevens, R. J., Norris, P. M., and Zhigilei, L. V., 2004. "Molecular-dynamics Study of thermal boundary resistance: Evidence of strong inelastic scattering transport channels". In Proceedings of IMECE 2004, ASME. Paper number IMECE2004-60334.

[23] Angadi, M. A., Watanabe, T., Bodapati, A., Xiao, X. C., Auciello, O., Carlisle, J. A., Eastman, J. A., Keblinski, P., Schelling, P. K., and Phillpot, S. R., 2006. "Thermal transport and grain boundary conductance in ultrananocrystalline diamond thin films". *Journal of Applied Physics,* **99**, p. 114301.

[24] McQuarrie, D. A., 2000. *Statistical Mechanics*. University Science Books, Sausalito.

[25] Puech, L., Bonfait, G., and Castaing, B., 1986. "Mobility of the ^{3}He solid-liquid interface: Experiment and theory". *Journal of Low Temperature Physics,* **62**, pp. 315–327.

[26] Barrat, J.-L., and Chiaruttini, F., 2003. "Kapitza resistance at the liquid-solid interface". *Molecular Physics,* **101**, pp. 1605–1610.

[27] Shenogin, S., Keblinski, P., Bedrov, D., and Smith, G. D., 2006. "Thermal relaxation and role of chemical functionalization in fullerene solutions". *Journal of Chemical Physics,* **124**, p. 014702.

[28] Ladd, A. J. C., Moran, B., and Hoover, W. G., 1986. "Lattice thermal conductivity: A comparison of molecular dynamics and anharmonic lattice dynamics". *Physical Review B,* **34**, pp. 5058–5064.

[29] Lukes, J., Li, D. Y., Liang, X.-G., and Tien, C.-L., 2000. "Molecular dynamics study of solid thin-film thermal conductivity". *Journal of Heat Transfer,* **122**, p. 536.

[30] McGaughey, A. J. H., and Kaviany, M., 2004. "Thermal conductivity decomposition and analysis using molecular dynamics simulations. Part I. Lennard-Jones argon". *International Journal of Heat and Mass Transfer,* **47**, p. 1783.

[31] McGaughey, A. J. H., and Kaviany, M., 2004. "Quantitative validation of the Boltzmann transport equation phonon thermal conductivity model under the single-mode relaxation time approximation". *Physical Review B,* **69**, p. 094303.

[32] McGaughey, A. J. H., Hussein, M. I., Landry, E. S., Kaviany, M., and Hulbert, G. M. Phonon Band Structure and Thermal Transport Correlation in a Layered Diatomic Crystal, to appear in *Physical Review B*.

[33] Schelling, P. K., Phillpot, S. R., and Kelinski, P., 2002. "Comparison of atomic-level simulation methods for computing thermal conductivity". *Physical Review B,* **65**, p. 144306.